MASTER THESIS

Numerical Calculation of the Efficiency of a Ratchet System

ラチェット機構における輸送効率の数値計算

Masaru Yoshiwara

吉原勝

(35102041)

Department of Physics,
Graduate School of Science and Engineering,
Aoyama Gakuin University

Supervisors: Kenn Kubo and Naomichi Hatano
指導教官：久保健・羽田野直道

2003

論　文　要　旨
(和　文)

提 出 年 度： **2003**
提　出　日： **2004/02/10**
専　　攻： 物理学
学 生 番 号： **35102041**
学 生 氏 名： 吉原勝
研究指導教員： 久保健　羽田野直道

（論文題目）
ラチェット機構における輸送効率の数値計算

（内容の要旨）

本研究では分子モーター（例えば筋収縮のアクチン・ミオシン系）のモデルのひとつであるラチェット機構の輸送効率を計算し、その空間周期、時間周期、温度への依存性について議論する。

ラチェットとは非対称な歯を持つ歯車とその回転を止める爪からなる機械であり、爪には歯車の回転を一方向に整流する能力がある。これにヒントを得て非対称な周期ポテンシャル中の粒子の熱運動を考える。熱ゆらぎによるブラウン運動、ポテンシャルの非対称性、外からのエネルギーの注入という３つの要素により分子モーターは一方向へ運動する。これが分子モーターのラチェットモデルである。エネルギーがどのように系に注入されるかによっていろいろなモデルが提案されているが、本研究では最も簡単な Stochastic ratchet model を用いる。

本研究で議論する輸送効率には二つの意味が考えられる。一つは単位時間当たりにどれだけ粒子が一方向へ進むかという意味での効率であり、もう一つは外から入力したエネルギーに対しどれだけ粒子が仕事を出力するかという意味での効率である。前者はスピード、後者はエネルギー効率と言い換えることができる。

まずスピードについて考えてみる。拡散距離が小さいと、粒子はポテンシャルの山を越えることができないし、また拡散距離が大きすぎれば、粒子は左右両側のポテンシャルの山を越えることになるので一方向へ進むスピードは遅くなる。つまり粒子が一方向へ速く進むには、ポテンシャルがオフの間にブラウン運動によって拡散する距離が、ポテンシャルの空間周期 L とおおむね等しくなる場合であると予想される。粒子の拡散距離は時間周期 t の平方根に比例することを考慮すれば、

$$L \approx \sqrt{Dt}$$

が満たされる時にスピードはピークを取ると考えられる。ここで D は拡散係数という温度に比例したパラメーターである。これは温度が高ければ粒子の拡散距離が大きくなり、低ければ拡散距離が小さくなることに対応している。以上を総合すれば粒子のスピードのピークは

$$L \approx \sqrt{D'Tt}$$

を満たすように推移して行くと考えられる。ここで $D = D'T$ とおいた。本研究のシミュレーションでこれが確かめられた。

つぎにエネルギー効率 η について考える。η を次式のように定義する。

$$\eta = W / E_{IN}$$

ここで W 、E_{IN} はそれぞれ系のする仕事、系への入力エネルギーである。まず W は粒子のスピードに比例すると考えられる。それは粒子のスピードが速いほど仕事も大きくなるためである。したがって上と同じ考察ができる。一方、E_{IN} については以下のように考察できる。E_{IN} はポテンシャルが粒子にする仕事と粒子がポテンシャルにする仕事の差である。このような考察から、

$$E_{in} \propto \sqrt{\tau T}$$

が得られ、エネルギー効率 η は有限の温度でピークを取ると予想される。我々はこの考察をシミュレーションにより確認する。

Academic Year of 2003, Submitted on February 25, 2004

Graduate School of Science and Engineering, Aoyama Gakuin University

Numerical Calculation of the Efficiency of a Ratchet System

Masaru Yoshiwara (35102041)
Department of Physics, Master Course
Supervisors: Kenn Kubo and Naomichi Hatano

We calculate the speed and the energy efficiency of the stochastic ratchet system, a model of a molecular motor. We show their dependence on the spatial period, the temporal period, and the temperature by carrying out an extensive Monte Carlo simulations.

The stochastic ratchet model is a system of Brownian particles in an oscillating asymmetrical potential, so-called the ratchet potential. The particles can move in one direction even when the time and space averages of all macroscopic forces and gradients are zero.

We first consider the speed of the particles. The particles cannot move over the potential teeth, if the diffusion distance $\sqrt{D\tau}$ is too small when compared with the spatial period L of the ratchet potential, where D is the diffusion coefficient and τ is the temporal period. On the other hand, the particles move over the potential teeth on both sides regardless of the potential asymmetry, when the diffusion distance is too large. The speed of the particle must be small in both cases. In order for the particles to progress quickly in one dimension, the diffusion distance must be comparable to the spatial period of the potential. Thus we have

$$L \approx \sqrt{D\tau}$$

as the optimal condition for the speed. We confirm this condition in our simulation.

We next consider the energy efficiency. We define the efficiency η as

$$\eta \equiv W / E_{\text{in}},$$

where W represents the work by the particle against a load potential, while E_{in} is the input energy. First, W should be proportional to the speed of the particle. Therefore, the same consideration as above applies here. On the other hand, E_{in} is the difference between the work by the ratchet potential to the particle and the work by the particle to the ratchet potential. After some consideration, we have

$$E_{\text{in}} \propto \sqrt{T\tau}.$$

Hence the energy efficiency is maximized at a temperature different from the one that maximizes the speed. We also confirm this in our simulation.

MASTER THESIS
Numerical Calculation of the Efficiency of a Ratchet System

Masaru Yoshiwara
(35102041)
Department of Physics,
Graduate School of Science and Engineering,
Aoyama Gakuin University
5-10-1 Fuchinobe, Sagamihara, Kanagawa 229-0006, Japan

Supervisors: Kubo Kenn and Hatano Naomichi

February 25, 2004

Abstract

We calculate the average velocity and the energy efficiency of the stochastic ratchet system, a model of the molecular motor. We show the dependence of the efficiency on the spatial period, the temporal period, and the temperature by carrying out an extensive Monte Carlo simulations.

We first argue that, in order for the particles to progress quickly in one direction, the diffusion distance must be comparable to the spatial period of the potential; in other words, we have $L \approx \sqrt{D\tau}$, as the optimal condition for the average velocity, where L is the spatial period of the ratchet potential, τ is the temporal period, and D is the diffusion constant. We confirm this condition in our simulation.

We next consider the energy efficiency. We argue that the energy efficiency is maximized at a temperature different from the one that maximizes the average velocity. We also confirm this in our simulation.

We find unfortunately that the efficiency of the stochastic ratchet system is quite lower than the experimental estimate of the myosin-actin system.

Contents

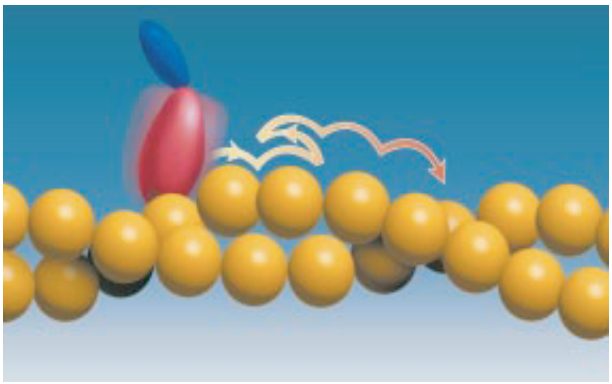

Figure 1: A myosin moves along actin filaments (from NIKKEI SCIENCE).

1 Introduction

1.1 Molecular motors

Molecular motors in biological systems are known to work with high efficiency in water at the room temperature. The work done by a molecule motor is from several times to dozen times greater than thermal energy. We hence cannot ignore influence of thermal fluctuation.

The myosin-actin system, for example, is a famous molecular motor (Fig.1). Actin filaments have a periodic structure with the period of about 5.5nm. It has been found experimentally that a myosin molecule moves along an actin filament in a fluctuating number of steps while one ATP (adenosine triphosphate) is used up [1]. This suggests that the myosin-actin system is strongly affected by thermal fluctuation. Since thermal fluctuation is usually a cause of incorrect operation, we try to make the influence small. Then, in spite of thermal fluctuation influencing the molecule motor, why can the molecular motor work efficiently? Do the principles of the molecular motor and the usual machine

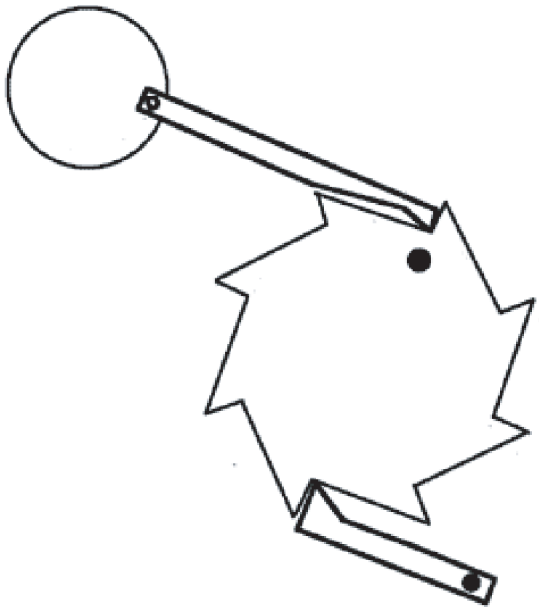

Figure 2: A ratchet wheel and a pawl (from http://www.automata.co.uk/).

differ? In order to answer these questions, motion induced by thermal fluctuation in ratchet systems have been investigated.

Many studies of the molecular motors have been carried out from the viewpoint of statistical physics [2, 3]. Much has been studied for ratchet models in order to determine how the directed motion emerges out of nonequilibrium fluctuation.

1.2 Ratchet systems

The ratchet is a machine which consists of a gear with asymmetrical teeth, and a pawl which restricts the rotation of the gear into one of the two directions as shown in Fig. 2. Taking a hint from this structure, we consider the thermal dynamics of Brownian particles in an oscillating asymmetrical potential. Brownian particles in an oscillating asymmetric potential can

on average drift in one direction even when the time and space averages of all macroscopic forces and gradients are zero.

Much has been studied for ratchet models to determine how the directed motion emerges out of nonequilibrium fluctuation. Most of the studies of the ratchet systems has been focused on analyses of the probability current [4]. Unfortunately, the energy efficiency has not been studied much, mostly because systematic methods of studying energetics have not been available for systems described by the Langevin equation. Recently, a method called stochastic energetics was proposed, in order to discuss the energy efficiency in the framework of the Langevin equation [5]. This method enables us to discuss the energetics of various ratchet systems [6, 7].

In the present thesis, we use the stochastic ratchet model among various ratchet models. We discuss two kinds of the efficiency of this model by carrying out an extensive simulation. One efficiency is the average velocity of the particle and the other is the energy efficiency. We emphasize that we become able to discuss the energy efficiency by introducing a load potential.

1.3 Outline of the thesis

In Section 2, we explain the stochastic ratchet model and define two types of its efficiency, the average velocity and the energy efficiency. The latter, in particular, is defined by introducing a load potential. We then discuss the average velocity and the energy efficiency qualitatively. We have $L \approx \sqrt{D\tau}$, as the optimal condition for the average velocity, where L is the spatial period of the ratchet potential, τ is the temporal period, and D is the diffusion coefficient. We also argue that the energy efficiency is maximized at a temperature different from the one

that maximizes the average velocity.

In Section 3, we explain our simulation procedure. In our simulation, the particle follows the Boltzmann distribution, when the potential is on. When the potential is off, on the other hand, the particle carries out a symmetrical movement. We give the physical constants and simulation parameters, taking the experiments into consideration.

In Section 4, we explain the details of our data analysis. In our data analysis, we take the sample average as well as the time average.

In Section 5, we discuss the results of our simulation and data analysis. We discuss the average velocity and the energy efficiency as functions of the temperature T and the potential frequency $\omega = 1/\tau$. We confirm that the results are in agreement with the arguments in Section 2.

In Section 6, we compare the results of our simulation with experimental data sand discuss the difference between the theoretical model calculation and experiments. We conclude that we cannot regard the stochastic ratchet model as a model of the myosin-actin system. The myosin-actin system uses the thermal energy much more effectively than the stochastic ratchet model.

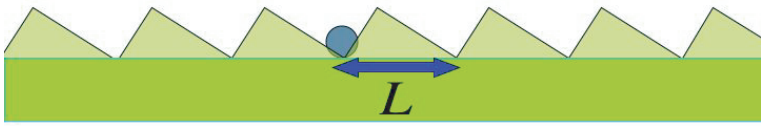

Figure 3: The piecewise linear potential $V(x)$ with a period L.

2 Stochastic ratchet model

2.1 Basic concepts

In this section, we explain the ratchet model studied in the present thesis. We consider diffusive motion in a periodic, anisotropic, piece-wise linear potential $V(x)$ as shown in Fig. 3; this is called a "ratchet" potential. If the potential did not change in time we would obtain as the stationary solution a Boltzmann distribution of the probability density,

$$P(x) = C \exp(-V(x)/k_B T). \tag{1}$$

In fact, we turn on and off the ratchet potential $V(x)$ periodically as in Fig. 4. The application of such a two-state noise can bring about a net flow of probability along the x axis, even though no macroscopic force is ever applied. The induced flux

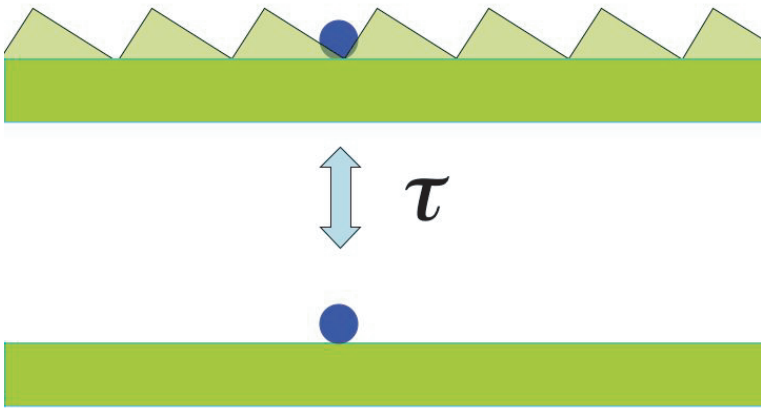

Figure 4: The oscillation of the potential with a temporal period τ.

can change, when we change parameters of the ratchet potential, such as the spatial and temporal periods and the potential height.

Particles diffuse in the ratchet potential due to thermal fluctuations. We can observe in Fig. 5 how the movement takes place; when the ratchet potential is on, the particles are concentrated near the bottoms of the potential valleys. When it is off, the diffusion produces a symmetrical dispersion of the particles. When it is turned on again, a portion of particles is displaced towards the right due to the asymmetry of the potential. Thus the probability flow is generated.

2.2 Average velocity

We now focus on two kinds of the efficiency of the ratchet system. We first consider the average velocity of the particle. The

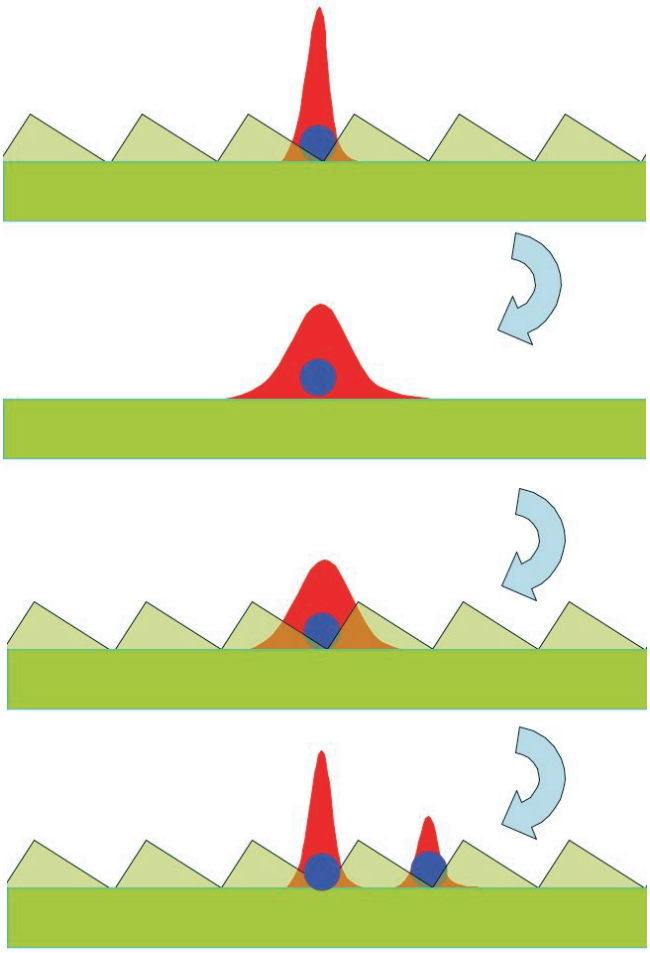

Figure 5: A portion of particles is displaced towards the right in the stochastic ratchet model.

diffusion distance of the particle within one cycle of the potential oscillation is proportional to the square root of the temporal period τ. The particle cannot go over the potential teeth if the diffusion distance $\sqrt{D\tau}$ is too small when compared with the spatial period L of the potential as in Fig. 6(a), where D is the diffusion coefficient. On the other hand, the particle goes over the potential teeth on both sides regardless of the potential asymmetry, when the diffusion distance is too large as in Fig. 6(b). The average velocity of the particle must be small in both cases. In order for the particle to progress quickly in one direction, the diffusion distance $\sqrt{D\tau}$ must be comparable to the spatial period L of the potential as in Fig 6(c).

Thus we have

$$L \approx \sqrt{D\tau}, \tag{2}$$

as the optimal condition for the average velocity. Since the coefficient D is proportional to the temperature T, we have

$$L \approx \sqrt{D'T\tau}, \tag{3}$$

where $D = D'T$. We below confirm this condition in our simulation.

2.3 Energy efficiency

Next, we consider the energy efficiency as another kind of the efficiency of the ratchet system. For this purpose, we introduce a load potential as in Fig. 7. The system converts the input energy into the work against the load. We define the energy efficiency η as

$$\eta = W/E_{\text{in}}, \tag{4}$$

where W represents the work per unit time by the particle against the load (Fig. 8(a)) and E_{in} is the input energy. The

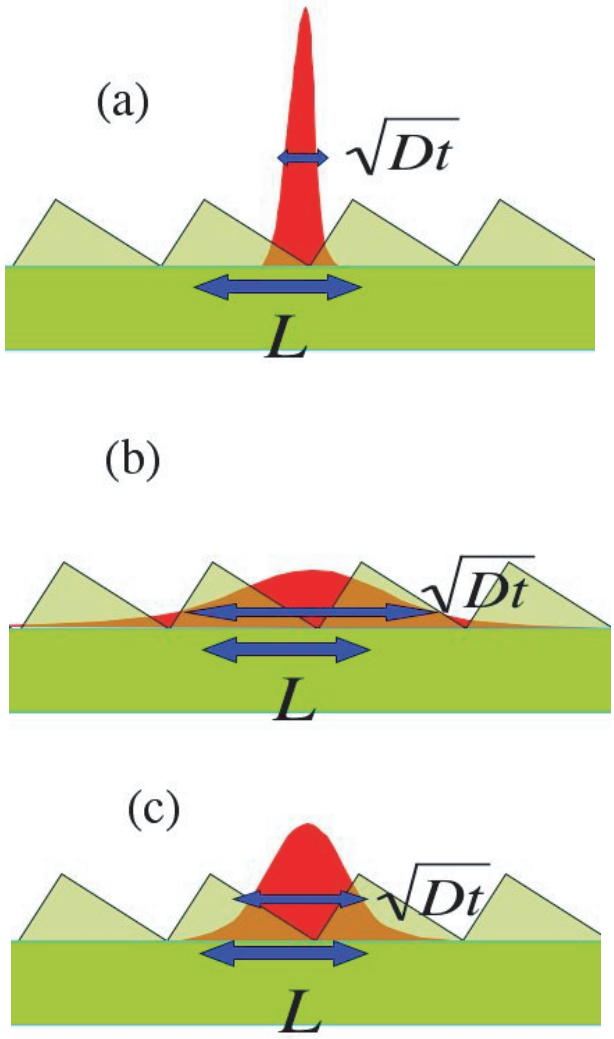

Figure 6: (a) The particle cannot go over the potential teeth if $L \gg \sqrt{D\tau}$. (b) The particle goes over the potential teeth on both sides if $L \ll \sqrt{D\tau}$. (c) The probability flow is expected to be maximal when the diffusion distance is comparable to the spatial period of the potential, namely $L \approx \sqrt{D\tau}$.

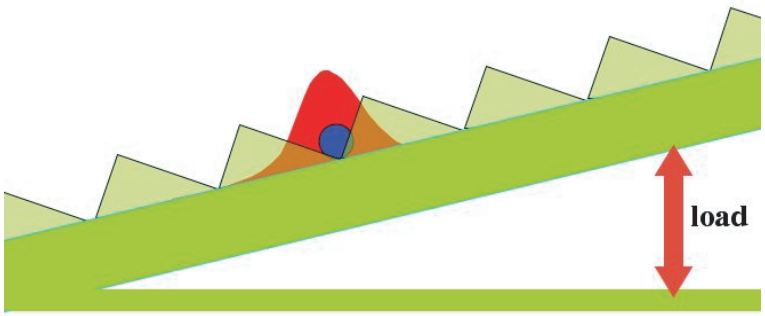

Figure 7: The ratchet system converts the input energy into the work against the load.

input energy per unit time, $E_{\rm in}$, is given by

$$E_{\rm in} = (E_A - E_B)/\tau, \tag{5}$$

where E_A is the work to the particle by the potential when we turn on the potential, and E_B is the work to the potential by the particle when we turn off the potential (Fig. 8(b)).

Let us roughly estimate W and $E_{\rm in}$. First, the output W should be proportional to the distance covered by the particle per unit time, namely the average velocity of the particle, if the load potential is not too steep. Therefore, the same consideration as in the previous subsection applies here. That is, the work W is maximized when the condition

$$L \approx \sqrt{D\tau} \tag{6}$$

is satisfied.

On the other hand, the input $E_{\rm in}$ can be estimated as follows. The diffusion distance $\sqrt{D'T\tau}$ is small at low temperatures. Since the particle moves slowly, E_A and E_B do not differ much, and hence $E_{\rm in}$ is small. Thus we have, for the input energy

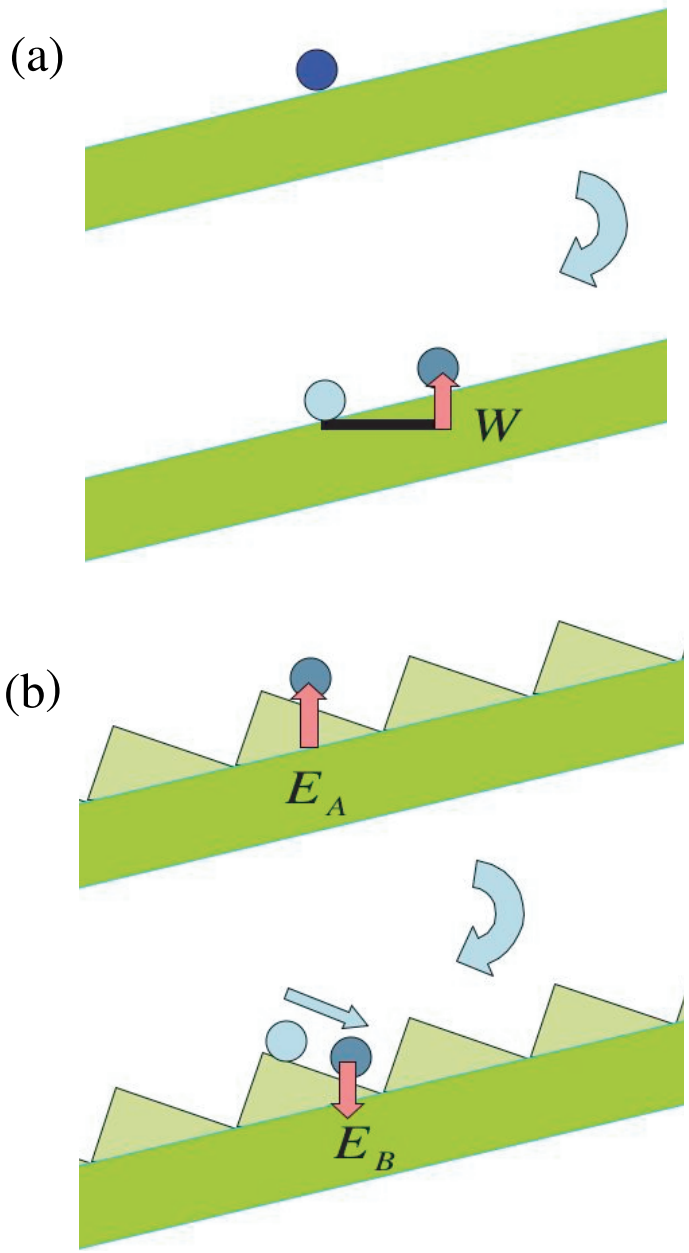

Figure 8: The definition of (a) the work W and (b) the input energy $E_{\rm in}$.

per unit time,

$$E_{\text{in}} \propto \frac{\sqrt{\tau T}}{\tau} = \sqrt{\frac{T}{\tau}} \tag{7}$$

for small τ and T. For large τ and T, the particle moves much, the energy difference $E_A - E_B$ reaches its limit, and hence

$$E_{\text{in}} \propto \frac{1}{\tau}. \tag{8}$$

In any case, the denominator of the energy efficiency is a decreasing function of τ and an increasing function of T.

By dividing W with E_{in} to obtain the energy efficiency η, the maximum of the numerator must be shifted towards a lager τ and a smaller T. We later see this in our simulation.

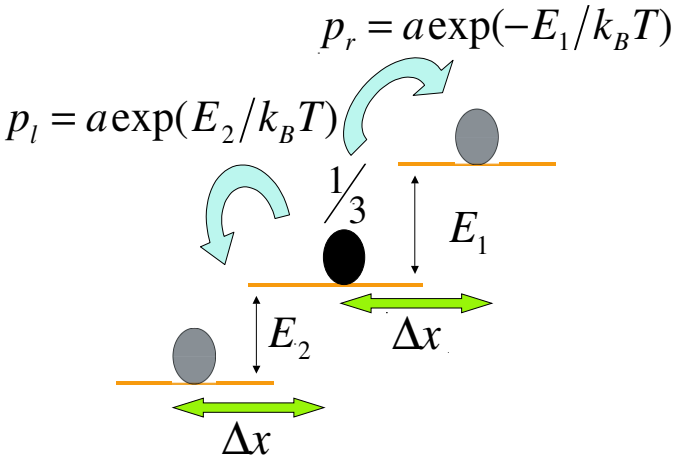

Figure 9: The probability of the particle movements in the case where the potential is on.

3 Simulation procedure

In this section, we explain our simulation procedure. A particle moves at every time step Δt on a one-dimensional lattice of mesh size Δx, according to the following rules.

A particle in the ratchet potential follows the Boltzmann distribution. When the potential is on, the probability $p_{\rm r}$ of climbing up the potential difference E_1 over the distance Δx is proportional to $\exp(-E_1/k_BT)$, while the probability $p_{\rm l}$ of climbing down E_2 is proportional to $\exp(E_2/k_BT)$, and the probability of staying is fixed to $1/3$ as is shown in Fig. 9. The normalization constant a for $p_{\rm r}$ and $p_{\rm l}$ is given by

$$a = \frac{2/3}{\exp(-E_1/k_BT) + \exp(E_2/k_BT)}. \tag{9}$$

When the potential is off, a particle carries out a symmetrical movement as in Fig. 10. Specifically, the probability of going

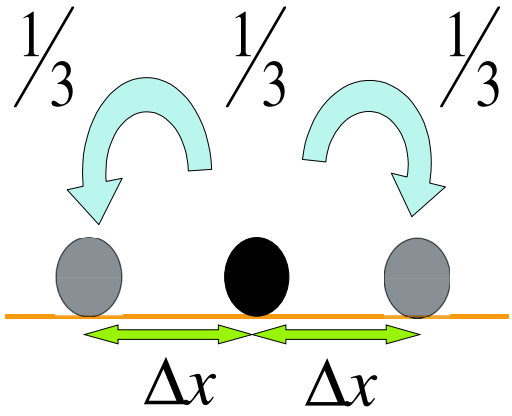

Figure 10: The probability of the particle movements in the case where the potential is off.

to the right over the distance Δx, the probability of going to the left over Δx, and the probability of staying are all 1/3. The probabilities defined in Fig. 9 are reduced to the ones in Fig. 10 for $E_1 = E_2 = 0$.

The temperature comes into the simulation as follows. The probability that a particle exists at a position x at time t, $P(x,t)$, is expressed in the form of the following master equation:

$$P(x, t+\Delta t) = \frac{1}{3}P(x+\Delta x, t) + \frac{1}{3}P(x-\Delta x, t) + \frac{1}{3}P(x,t), \quad (10)$$

or

$$\frac{P(x,t+\Delta t) - P(x,t)}{\Delta t} = \frac{1}{3}\frac{(\Delta x)^2}{\Delta t}\frac{P(x+\Delta x,t) + P(x-\Delta x,t) - 2P(x,t)}{(\Delta x)^2}. \quad (11)$$

By taking the limits $\Delta t \to 0$ and $\Delta x \to 0$, Eq. (11) is reduced

to the diffusion equation

$$\frac{\partial P}{\partial t} = D\frac{\partial^2 P}{\partial x^2}, \tag{12}$$

where the diffusion coefficient $D = k_B T/\zeta$ is related to the transition probability $1/3$ as

$$\frac{1}{3} = \frac{\Delta t}{(\Delta x)^2} D = \frac{\Delta t}{(\Delta x)^2}\frac{k_B}{\zeta} T. \tag{13}$$

Here, T is the temperature, k_B is the Boltzmann constant, and ζ is the viscous coefficient. By fixing Δx, we can thus change the temperature T by simply changing Δt:

$$k_B T = \frac{1}{3}\frac{\zeta(\Delta x)^2}{\Delta t}. \tag{14}$$

We now explain the outline of the simulation. We carried out the simulation twice; once without the load potential, and once with it. We calculate the average velocity from the former, and the energy efficiency η from the latter.

We put all N particles at the origin in the beginning and let them diffuse. The simulation begins when the potential is off. The potential is turned on at time $t = \tau/2$, turned off at time $t = \tau$, and so on. We continued the oscillation until $t = 1.5 \times 10^5 \tau$. We varied the temporal period in the range $10^{-8}\text{s} \leq \tau \leq 10^{-7}\text{s}$. The time scale of the fluctuation of the actin structure is known from experiments [9] to be about $10^{-9} \sim 10^{-3}$s. Unfortunately, we did not have time to cover the entire range in this thesis. We varied the temperature near the room temperature, namely $100\text{K} \leq T \leq 800\text{K}$.

We set the simulation constants as in Table 1. We determined the simulation parameters as follows. The coupling constant K

Physical Constants	
Boltzmann constant k_B	1.380658×10^{-23}J/K
Viscous coefficient ζ	$90\text{pN} \cdot \text{ns/nm}$
Joule per electron volt	$1.6021892 \times 10^{-19}$Je/V
Simulation Parameters	
Potential height	2.56×10^{-1}eV
Step distance Δx	0.1nm
Spatial period L	5.4nm
Particle number N	100
Load gradient l	1.8×10^{-4}eV/m

Table 1: The physical constants and the parameters in our simulation.

(which indicates the ease of the chemical reaction between the myosin molecule and the actin filament) is known from experiments [9] to be about 10^4mol^{-1}. The quantity $k_BT \ln K$ is the free-energy difference between the state where the myosin and the actin is connected by a chemical bond and the state where they are disconnected. We regard the difference of the free energy as the potential difference between the two states. Thus the potential height is estimated as $k_BT \ln K \approx 9k_BT$. We hence set the potential height as $9k_BT \approx 2.56 \times 10^{-1}$eV, by setting $T = 298$K.

Experiments show that the spatial period of the actin filament is about 5.5nm. In order to make the discretization error small, we put $\Delta x = 0.1$nm. We set the ratio between the distance from the peak to the left bottom and the peak to the right bottom as $1 : 8$, in order to emphasize the asymmetry of the potential so that the particle cannot go over the potential teeth easily for large τ. Thus the distance from the peak to the left bottom is set to $6\Delta x = 0.6$nm, and the peak to the right bottom to $48\Delta x = 4.8$nm; hence $L = 54\Delta x = 5.4$nm

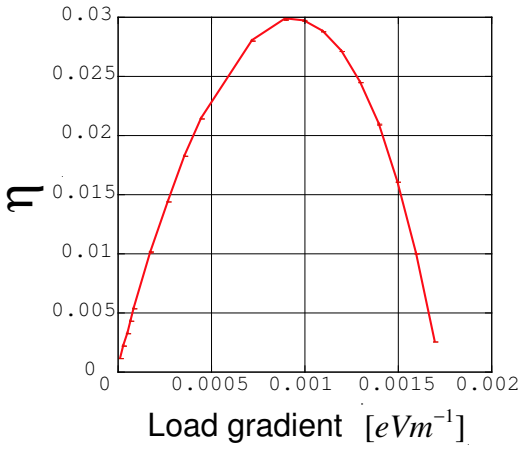

Figure 11: The efficiency η as a function of the load gradient for $T = 300$K, $\omega = 1/\tau = 1.0 \times 10^8 \mathrm{s}^{-1}$.

The gradient of the load potential, l, must be smaller than the potential gradient. We decide the load gradient so as not to let the particles climb down the load potential for any temporal periods and temperatures. For the purpose, we preliminarily carried out a simulation and evaluated the energy efficiency, at a fixed parameter set; see Fig. 11. Taking the margin, we set $l = 1.8 \times 10^{-4}$eV/m.

4 Data Analysis

We explain in this section the details of our data analysis [8]. First, we explain our choice of data series.

After each temporal period τ, we took the sample average with respect to the N particles:

$$\langle v \rangle_t = \frac{1}{N} \sum_{i=1}^{N} \frac{x_i(t)}{t}, \tag{15}$$

$$\langle w \rangle_t = \frac{l}{N} \sum_{i=1}^{N} \frac{x_i(t)}{t}, \tag{16}$$

$$\tilde{E}_{A,i}(t) = \sum_{t_0=\frac{1}{2}\tau,\frac{3}{2}\tau,\cdots}^{t-\frac{\tau}{2}} E_{A,i}(t_0), \tag{17}$$

$$\tilde{E}_{B,i}(t) = \sum_{t_0=\tau,2\tau,\cdots}^{t} E_{B,i}(t_0), \tag{18}$$

$$\langle e_{\rm in} \rangle_t = \frac{1}{N} \sum_{i=1}^{N} \frac{\tilde{E}_{A,i}(t) - \tilde{E}_{B,i}(t)}{t}, \tag{19}$$

where $x_i(t)$ is the position of the particle i at time t, l is the load gradient, $E_{A,i}(t_0)$ is the work to the particle i at the time t_0 by the potential when we turn on the potential and $E_{B,i}(t_0)$ is the work to the potential by the particle i at the time t_0 when we turn off the potential (Fig. 8). Note that we calculate Eq. (15) from the data without the load potential, whereas Eqs. (16)-(19) from the data with it. The time dependence of the averages is plotted in Fig. 12 with their statistical errors. We see that the initial relaxation remains until $t \approx 0.3 \times 10^5 \tau$. Hence we discarded the first 1/5 of the data series, which leaves

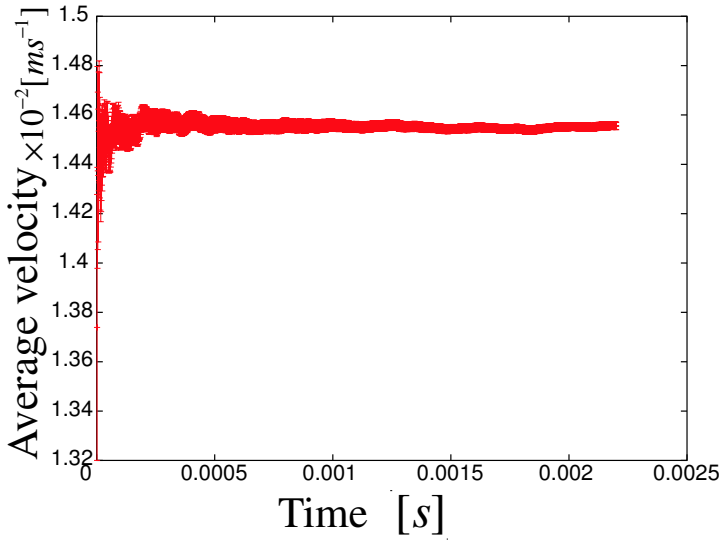
Average velocity $\times 10^{-2}[ms^{-1}]$
1.5
1.48
1.46
1.44
1.42
1.4
1.38
1.36
1.34
1.32
0
0.0005
0.001
0.0015
0.002
0.0025
Time $[s]$

(a)

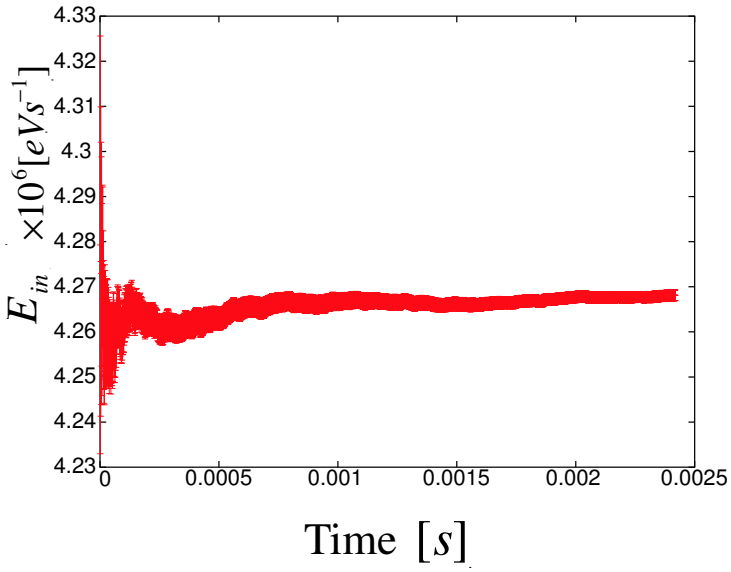
E_{in} $\times 10^{6}[eVs^{-1}]$
4.33
4.32
4.31
4.3
4.29
4.28
4.27
4.26
4.25
4.24
4.23
0
0.0005
0.001
0.0015
0.002
0.0025
Time $[s]$

(b)

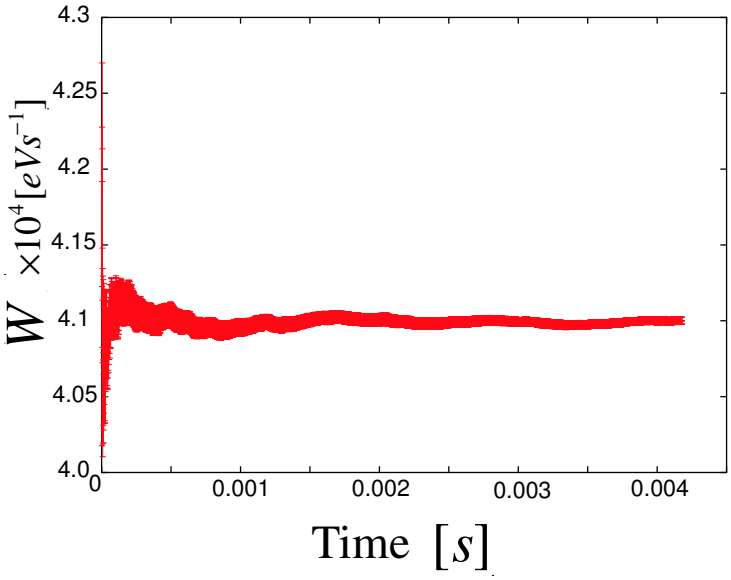

(c)

Figure 12: The initial relaxation of the expected values. (a) The average velocity as a function of the time for $T = 100\text{K}$ and $\omega = 1/\tau = 9.0 \times 10^7 \text{s}^{-1}$. (b) The input E_{in} as a function of the time for $T = 300\text{K}$ and $\omega = 1/\tau = 9.0 \times 10^7 \text{s}^{-1}$. (c) The output W as a function of the time for $T = 200\text{K}$ and $\omega = 1/\tau = 8.0 \times 10^7 \text{s}^{-1}$.

us 1.2×10^5 pieces of data of each quantity. These data, however, have a temporal autocorrelation. In order to use independent data, we chose a point every 150 data, extracting 800 data points of each quantity.

The final average velocity V and its statical error ΔV are calculated as follows:

$$V = \frac{1}{800}{\sum_t}'\langle v\rangle_t, \tag{20}$$

$$\Delta V = \frac{1}{\sqrt{800(800-1)}}\sqrt{{\sum_t}'\left(\langle v\rangle_t - V\right)^2}, \tag{21}$$

where ${\sum_t}'$ denotes the sum of 800 extracted data of $\langle v\rangle_t$.

Similarly, we have the output W and its statical error ΔW as

$$W = \frac{1}{800}{\sum_t}'\langle w\rangle_t, \tag{22}$$

$$\Delta W = \frac{1}{\sqrt{800(800-1)}}\sqrt{{\sum_t}'\left(\langle w\rangle_t - W\right)^2}, \tag{23}$$

and the input $E_{\rm in}$ and its statical error $\Delta E_{\rm in}$ as

$$E_{\rm in} = \frac{1}{800}{\sum_t}'\langle e_{\rm in}\rangle_t, \tag{24}$$

$$\Delta E_{\rm in} = \frac{1}{\sqrt{800(800-1)}}\sqrt{{\sum_t}'\left(\langle e_{\rm in}\rangle_t - E_{\rm in}\right)^2}. \tag{25}$$

The average energy efficiency was obtained as follows. We first computed the quantity

$$\tilde{\eta}_t = \frac{\langle w\rangle_t}{\langle e_{\rm in}\rangle_t} \tag{26}$$

at every temporal period. The final estimate of the energy efficiency η and its statical error $\Delta\eta$ are calculated as

$$\eta = \frac{1}{800}\sum_t{}'\tilde{\eta}_t. \tag{27}$$

$$\Delta\eta = \frac{1}{\sqrt{800(800-1)}}\sqrt{\sum_t{}'\left(\tilde{\eta}_t-\eta\right)^2}. \tag{28}$$

5 Simulation results

We examine here two types of the efficiency defined in Section 2.

5.1 Average velocity

We first find in our simulation that the average velocity of the particle is maximized at a finite temperature. We argued in Section 2 that the the maximum average velocity is achieved when

$$L \approx \sqrt{D\tau} \approx \sqrt{D'\tau T} \propto \sqrt{T/\omega}, \tag{29}$$

where ω is the frequency of the potential oscillation, $\omega = 1/\tau$. Hence the optimal frequency $\omega_{\rm opt}$ and the optimal temperature $T_{\rm opt}$ should be related in the form

$$T_{\rm opt} \propto \omega_{\rm opt}, \tag{30}$$

when we fix the spatial period L. We note in Fig. 13 that a ridge indeed runs diagonally on the ω-T plane.

Let us plot in Fig. 14 how the ridge runs. We first look for the maximum average velocity at a fixed temperature. For example, the frequency giving the maximum average velocity is $\omega_{\rm opt} = 4 \times 10^7 {\rm s}^{-1}$ at $T = 100{\rm K}$. We also plot the error as half the mesh size. For example, we have the data points for $\omega = 3 \times 10^7 {\rm s}^{-1}$ and $\omega = 5 \times 10^7 {\rm s}^{-1}$ besides the data for $\omega_{\rm opt} = 4 \times 10^7 {\rm s}^{-1}$, and hence $\Delta\omega_{\rm opt} = 0.5 \times 10^7 {\rm s}^{-1}$. Likewise, the temperature giving the maximum average velocity is $T_{\rm opt} = 330{\rm K}$ at $\omega = 2 \times 10^7 {\rm s}^{-1}$. We see in Fig. 14 that the maximum average velocity indeed runs diagonally on the ω-T plane.

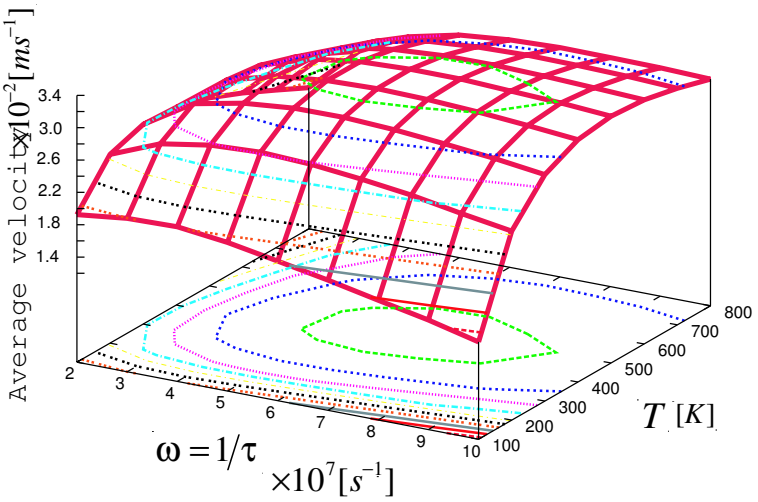

Figure 13: The average velocity of the particle as a function of the temperature T and the frequency ω.

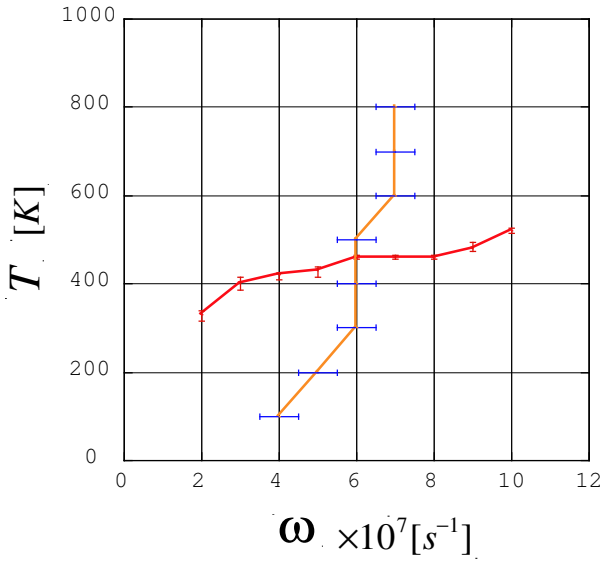

Figure 14: The maximum average velocity as a function of the frequency ω at each fixed temperature T (orange line) and as a function of the temperature T at each fixed frequency ω (red line).

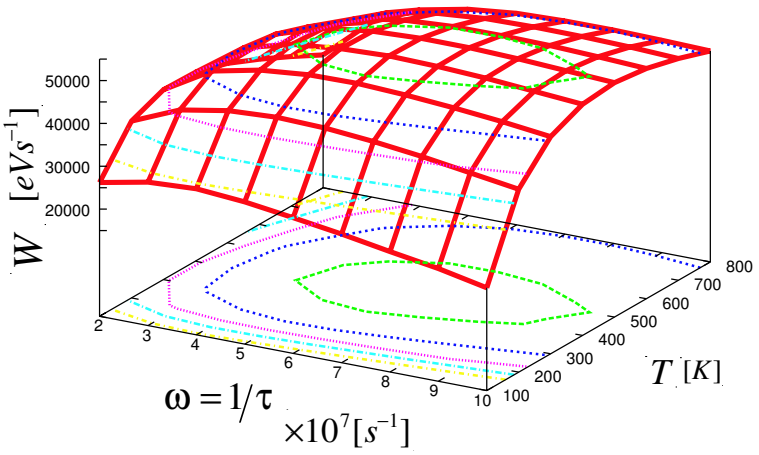

Figure 15: The work per unit time as a function of the temperature T and the frequency ω.

5.2 Energy efficiency

Next, we consider the energy efficiency. In Section 2, we defined the efficiency η as

$$\eta = W/E_{\text{in}}. \tag{31}$$

The work W is maximized at a finite temperature as in Fig. 15. We carried out the same data processing as we did to obtain Fig. 14 from Fig. 13, and obtained Fig. 16 from Fig. 15.

We see in Fig. 16 that a ridge of the maximum work runs diagonally on the ω-T plane. This behavior is the same as that of the average velocity, as we discussed in Section 2.3.

On the other hand, the input E_{in} is a decreasing function of the temporal period τ as in Fig. 17. This is also consistent with our argument in Section 2.3.

The energy efficiency is hence maximized at a temperature different from the one that maximizes the average velocity as is seen when we compare Figs. 13 and 18. The ridge of η is

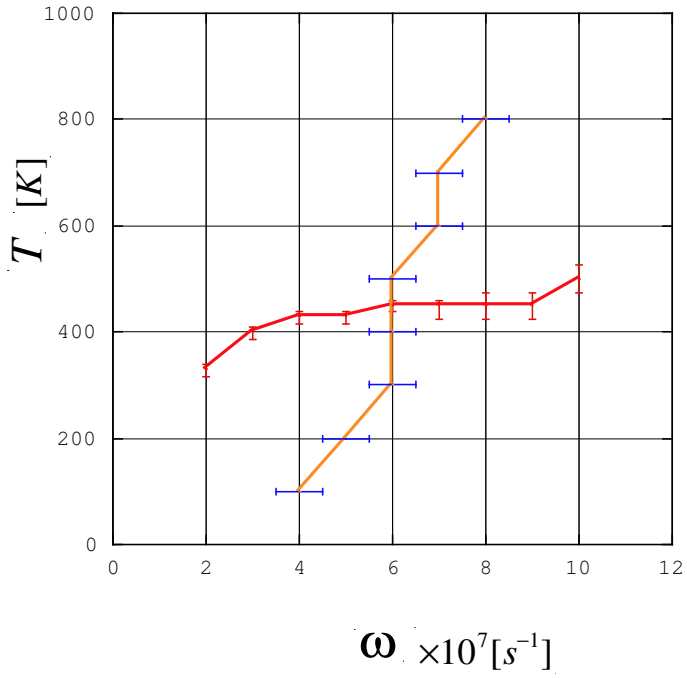

Figure 16: The maximum work per unit time W as a function of the frequency ω at each fixed temperature T (orange line) and as a function of the temperature T at each fixed frequency ω (red line).

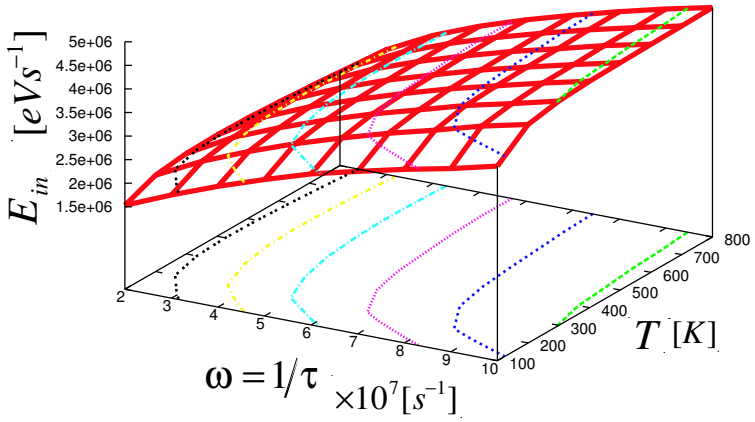

Figure 17: The input energy per unit time as a function of the temperature T and the frequency ω.

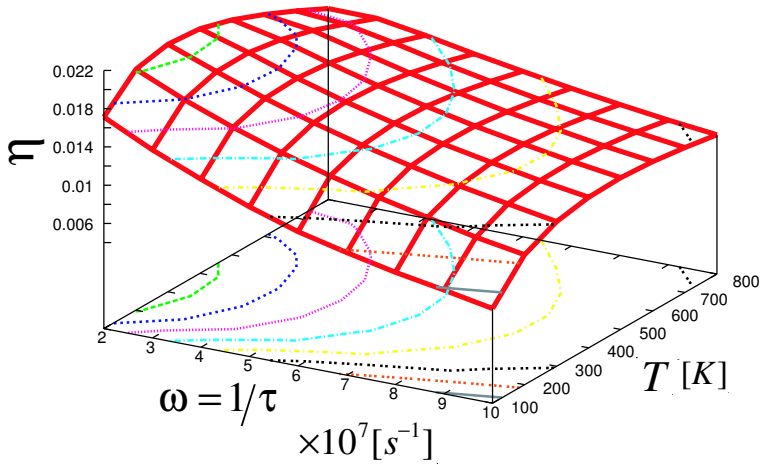

Figure 18: The energy efficiency as a function of the temperatures T and the frequency ω.

plotted in Fig. 19. We see when we compare Figs. 14 and 19 that the maximum shifted. Furthermore, the efficiency η is also an increasing function of the temporal period τ as in Fig 18, because $E_{\rm in}$ is a decreasing function of the temporal period τ whereas W is maximized at a finite frequency.

We see in Fig. 18 that the maximum of the energy efficiency η at a fixed temperature vanishes. Let us consider the behavior of the efficiency η in the limit $\tau \to \infty$, or $\omega \to 0$. The output W should be negative in $\tau \to \infty$, because the particle simply climbs down the load potential when the ratchet potential does not oscillate. On the other hand, the input $E_{\rm in}$ should be 0 in $\tau \to \infty$, since the input occurs only when the potential changes in time. Consequently, the efficiency η should be $-\infty$ in $\tau \to \infty$. Therefore, η must be maximized at a finite temporal period τ. Unfortunately, the maximum is not included in our parameter range of ω.

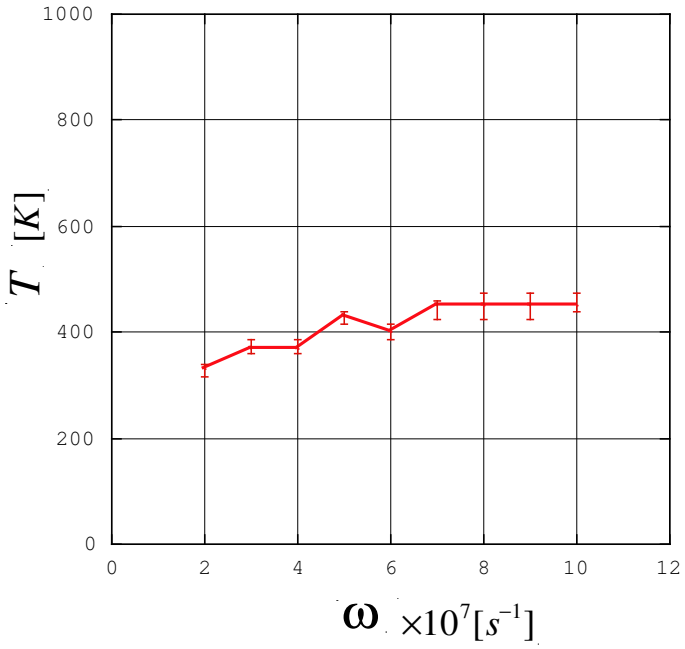

Figure 19: The maximum energy efficiency as a function of the temperature T at each fixed frequency ω.

6 Conclusions

We calculated the average velocity and the energy efficiency in the stochastic ratchet model. Consequently, we have

$$L \approx \sqrt{D\tau}, \tag{32}$$

as the optimal condition for the average velocity. We confirm this condition in our simulation. Furthermore, we confirm that the energy efficiency is maximized at a temperature different from the one that maximizes the average velocity.

We here compare our simulation with the experimental data given in Ref. [9]. We conclude that the myosin-actin system uses the thermal energy much more effectively than the stochastic ratchet model. Unfortunately, we cannot regard the stochastic ratchet model as a model of the myosin-actin system as we below compare the average velocity and the energy efficiency.

The average velocity in our simulation ($\approx 10^{-2}$m/s) is much greater than the experimental estimate ($\approx 10^{-6}$m/s). The output W in our simulation ($\approx 10^{4}$eV/s) is also much greater than the experimental estimate (≈ 5eV/s). The input $E_{\rm in}$ in our simulation ($\approx 10^{6}$eV/s) is again greater than the experimental estimate (≈ 10eV/s). The efficiency $\eta = W/E_{\rm in}$ in our simulation (≈ 0.01), however, is smaller than the experimental estimate ($\approx 0.4 \sim 0.5$).

We discuss why the stochastic ratchet model is inconsistent with the myosin-actin system greatly. The myosin-actin system produces a little output from a little input. On the other hand, the particle produces much output from much input in the stochastic ratchet model. In the stochastic ratchet model, whenever the potential is on for $\tau/2 \approx 10^{-8}$s, the particle often goes over the potential teeth. In the real system, however, the

myosin fluctuates much less frequently, namely of the frequency $\sim 10^{-3}$s.

The difference in the efficiency between the ratchet model and the myosin-actin system becomes clear when we compare the input energy with thermal energy. The input energy is from several times to dozen times greater than thermal energy in the myosin-actin system. In the stochastic ratchet model, the input energy $E_{\rm in}$ is much greater than thermal energy. In other words, the particle does not use the thermal energy effectively in the stochastic ratchet model. The particle uses only the input energy, which is wasted so much.

The stochastic ratchet model, unfortunately, cannot describe the real myosin-actin system. Recently, the energetics of various ratchet model are studied [5], including a ratchet model of higher efficiency [6]. In the near future, we hope that more controlled experiments will be available, where we can know the dependence of the energy efficiency on the diffusion coefficient and the protein fluctuation. Then we will be able to know what model is appropriate for molecular motors.

References

[1] T. Yanagida, *"Biological Molecular Motor"* (Iwanami Shoten, 2002)

[2] R.D. Atsumian and M. Bier, Phys. Rev. Lett. **72**, 1766 (1994)

[3] F. Jülicher, A. Ajdari and J. Prost, Rev. Mod. Phys. **69**, 1269 (1997)

[4] M.O. Magnasco, Phys. Rev. Lett. **71**, 1477 (1993)

[5] K. Sekimoto, J. Phys. Soc. Jpn. **66**, 1234 (1997)

[6] H. Kamegawa, T. Hondou and F. Takagi, Phys. Rev. Lett. **80**, 5251 (1998)

[7] F. Takagi and T. Hondou, Phys. Rev. E **60**, 4954 (1999)

[8] T. Awaya, *"Data Analysis"* (Gakkai Shuppan Center, 1983)

[9] The Biophysical Society of Japan, *"The Imaging of the Nano-picospace"* (Yoshioka Shoten, 1997)